ON THE MEASUREMENTS OF THE SKIN FRICTION IN 3-D FLOWS. APPLICATION TO A COMPLETE 3-D SHEAR LAYER FLOW.†

G. Iuso
Department of Aerospace Engineering, Politecnico di Torino (Italy)
M.S. Oggiano
Fluidynamics Research Centre of CNR, Torino (Italy)
S. De Ponte
Department of Aerospace Engineering, Politecnico di Milano (Italy)

Abstract

Two different techniques based on different working principles, and suitable for measuring wall shear stress in 3-D boundary layer have been investigated.

Triangular block pressure probe and hot-wire wall probe have been accurately calibrated in a channel flow and an application is given for a complex 3-D shear flow generated in the same calibration channel, mounting a cylinder from wall to wall in the center of the test section. Oil flow visualization and power spectrum are also performed.

1. Introduction

Improvements of aerodynamic performances of a modern aircraft require an accurate configuration optimization; one of the goal in this contest is an accurate prediction of the friction drag[1]. The evaluation of the wall shear stress is also one of the main object in order to predict and understand flow fields that develop near and far from the wall; precious are in fact the informations given for: transitional regimes, analysis of 2-D and especially 3-D separations[2], complex flow on delta wing, slender body and body of revolution at incidence.

Moreover the knowledge of the wall shear stress is also crucial for numerical validation codes because of the velocity, u_τ, and lenght, l_τ, scales are deduced from the wall shear stress and the kinematic viscosity.

The possibility to measure the wall shear stress in severe conditions (3-D boundary layer with strong pressure gradient) is an ambitious aim.

In the 2-D case very well arranged techniques are established, for exemple Preston tubes[3], obstacles[4], heated elements[5,6,7], whose application is related to the assumption of validity of some universal laws (law of the wall and Reynolds analogy). Direct measurements are also recommended using balances[4], even if in this case under strong pressure gradient conditions there could be serious problems.

Measurements in 3-D flows are very difficult not only for the complexity of the flow, but also whether for the extension of the 2-D relations to the 3-D case (law-wall technique), that is quite doubtful, or for the presence of both longitudinal and transversal pressure gradients. Triangular block probes [8,9,10,11], heated elements[7,12,13], double Preston[14] have been extensively used. In[10] has been shown the application limits of the triangular pressure probe, comparing the results from measurements with a well established law of the wall for 3-D boundary layer, while in[11] and[13] are analysed some geometric parameters that could influence the calibration curves.

The purpose of this work is to compare the performances of two kinds of probes suitable for 3-D measurements whose working principles are completely different, and to verify if a channel calibration technique, where three-dimensional conditions are simulated rotating the probes respect to the main flow in the duct, is sufficiently reliable or not.

Omnidirectional triangular pressure and hot-wire wall probes are calibrated in a channel flow and used to measure the wall shear stress vector field on the channel wall, originating a 3-D complex shear flow by inserting a cylinder ($\phi = 88mm$) between the channel walls.

Comparisons are also made with oil flow visualization of the skin friction field.

Finally evidences of unsteadyness in the flow around the cylinder is also given from hot wire wall probes.

2. Experimental arrangements, probes and calibration techniques

2.1 Calibration apparatus

The calibrations have been carried out in a channel shown in Fig.1, whose details are repoprted in [11,15].

Briefly, it is formed by a duct, $6m$ long, and having rectangular cross section with aspect ratio of 14. The test section is placed $4m$ downstream the contraction, with an area ratio of 20; a AC motor, driven by an inverter, having a centrifugal blower on his shaft, allows to change the Reynolds number from 1000 to 60.000 $[Re = (U_{max}2H)/\nu]$. The flow in the test section has been attentively tested[11] in order to be sure to have a fully developed flow.

In a channel flow the shear stress is related to the pressure drop, and in particular at the wall results:

$$\tau_w = \left| \frac{dP}{dx} \right| \frac{H}{2}$$

where H is the channel height, equal to $20mm$.

During the calibrations the probes have been mounted on a rotating disc placed in the center of the test section, that have allowed a fully rotation of the probes respect to the longitudinal channel axis, with an accuracy of 0.1 degree.

† The research has been supported by CNR (Italian National Research Council) and MURST (Italian Ministry of University and Scientifical Technological Research)

2.2 Triangular block pressure probes.

Nituch and Rainbird[8] first suggested to use such a probe for measurements in 3-D flow; also Dexter[9] used extensively this kind of sensor.

The probe, sketched in Fig.2, is made of two thin triangular copper foil glued togheter.

Making use of the three measured pressures, it is possible to evaluate the directional calibration functions:

$$F(\delta) = \frac{P_1 - P_3}{P_1 - P_2}$$

$$G(\delta) = \frac{| P_1 - \frac{P_2+P_3}{2} |}{| P_1 - \frac{P_2+P_3}{2} |_{\delta=0}}$$

in each angular sector of 60° as shown in Tab.1, according to the pressure hole indice. The angle δ is defined between the wall shear stress direction and the probe axis.

A skin friction calibration curve is also necessary for each side; according to similar calibration parameter, introduced by Patel[3]:

$$X^* = log_{10} \frac{| P_1 - (P_2 + P_3)/2 |_{\delta=0} h^2}{\rho \nu^2}$$

$$Y^* = log_{10} \frac{\tau_w h^2}{\rho \nu^2}$$

where h is the probe height, is possible give rise to the function $Y^* = Y^*(X^*)$ that is universal for a Preston tube in 2-D case.

Once the three pressures are measaured, the function $F(\delta)$ allows to evaluate the direction δ of the wall shear stress and then $G(\delta)$ gives the value of $| P_1 - \frac{P_2+P_3}{2} |_{\delta=0}$; at this point is also possible to calculate the X^* value and finally, from the skin friction calibration curve, the value of τ_w.

In Figs. 3, 4 and 5 the calibration curves of four triangular block pressure probes, nominally equal, are shown. As it can be seen the directional functions $F(\delta)$ and $G(\delta)$ are not exactly the same for each probe. The reason why this drawback happens is due to some unavoidable geometrical differences between the probes and to the zero positioning uncertainty, that could have a shift effect.

Also the skin friction calibration curves display the same problem, but in this case, probably, are not geometrical differences the responsable, but the relative positioning between each pressure hole and the triangular block. In fact this parameter could influence the sensitivity of each side of each probe.

A better repetitive set calibration curves is expected, improving the manufacturing technique.

Finally an error estimation lead considering the whole calibration set to an inaccuracy of 3° for the wall shear stress direction and in about 7% for the modulus of the skin friction.

2.3 Hot wire wall probes.

The probe, whose basic configuration is reported in[12,13], consists of a cylindrical base made of "plexiglas", on which

	F	G	X^*
$0° \le \delta \le 60°$	$\frac{P_1 - P_3}{P_1 - P_2}$	$\frac{\left[P_1 - \frac{P_2+P_3}{2}\right]_\delta}{\left[P_1 - \frac{P_2+P_3}{2}\right]_{\delta=0}}$	$log_{10} \frac{\left[P_1 - \frac{P_2+P_3}{2}\right]_{\delta=0} h^2}{\rho \nu^2}$
$60° \le \delta \le 120°$	$\frac{P_3 - P_1}{P_3 - P_2}$	$\frac{\left[P_3 - \frac{P_1+P_2}{2}\right]_\delta}{\left[P_3 - \frac{P_1+P_2}{2}\right]_{\delta=0}}$	$log_{10} \frac{\left[P_3 - \frac{P_1+P_2}{2}\right]_{\delta=0} h^2}{\rho \nu^2}$
$120° \le \delta \le 180°$	$\frac{P_3 - P_2}{P_3 - P_1}$	$\frac{\left[P_3 - \frac{P_1+P_2}{2}\right]_\delta}{\left[P_3 - \frac{P_1+P_2}{2}\right]_{\delta=0}}$	$log_{10} \frac{\left[P_3 - \frac{P_1+P_2}{2}\right]_{\delta=0} h^2}{\rho \nu^2}$
$180° \le \delta \le 240°$	$\frac{P_2 - P_3}{P_2 - P_1}$	$\frac{\left[P_2 - \frac{P_3+P_1}{2}\right]_\delta}{\left[P_2 - \frac{P_3+P_1}{2}\right]_{\delta=0}}$	$log_{10} \frac{\left[P_2 - \frac{P_3+P_1}{2}\right]_{\delta=0} h^2}{\rho \nu^2}$
$240° \le \delta \le 300°$	$\frac{P_2 - P_1}{P_2 - P_3}$	$\frac{\left[P_2 - \frac{P_3+P_1}{2}\right]_\delta}{\left[P_2 - \frac{P_3+P_1}{2}\right]_{\delta=0}}$	$log_{10} \frac{\left[P_2 - \frac{P_3+P_1}{2}\right]_{\delta=0} h^2}{\rho \nu^2}$
$300° \le \delta \le 360°$	$\frac{P_1 - P_2}{P_1 - P_3}$	$\frac{\left[P_1 - \frac{P_2+P_3}{2}\right]_\delta}{\left[P_1 - \frac{P_2+P_3}{2}\right]_{\delta=0}}$	$log_{10} \frac{\left[P_1 - \frac{P_2+P_3}{2}\right]_{\delta=0} h^2}{\rho \nu^2}$

Table 1. - Triangular block pressure probe set calibration.

two hot wires are flush-mounted and soldered to four steel prongs, in a V configuration (see Fig.6). In the middle position of the wire is present a circular cavity that confers a much higher sensitivity[13]. The gauge in such a fashion is flush-mounted on the rotating disc allowing its calibration in the channel and in a second step the measurements. The sensing element is a "Dantec" standard wire made of tungsten gold plated and having $5\mu m$ diameter and $1.8mm$ lenght.

Such a probe operates in a constant temperature anemometer with an overheat ratio equal to 0.72, and displaying an high frequency response that is of the same order of a classical hot wire; from the square wave test it results in 30 kHz.

The working principle is based on the measurement of velocity induced in the cavity by the skin friction; due to the fact that the cavity itself is rather small, it does not affect too much the stress field, but the flow at the upper edge of the cavity is related to the skin friction. In this way it is possible that the overall cooling of the wire is rather larger than pure conduction as in the case of wall films and there is not strong dependance on Reynolds analogy.

The probe will therefore have a similar calibration both

Such a probe operates in a constant temperature anemometer with an overheat ratio equal to 0.72, and displaying an high frequency response that is of the same order of a classical hot wire; from the square wave test it results in 30 kHz.

The working principle is based on the measurement of velocity induced in the cavity by the skin friction; due to the fact that the cavity itself is rather small, it does not affect too much the stress field, but the flow at the upper edge of the cavity is related to the skin friction. In this way it is possible that the overall cooling of the wire is rather larger than pure conduction as in the case of wall films and there is not strong dependance on Reynolds analogy.

The probe will therefore have a similar calibration both in laminar and turbulent flow.

On the other hand, the sensitivity is quite higher than wall films, and it is a significant advantage.

Such a probe results to be sensitive to temperature variations and quite insensitive to any influence of pressure gradient except for cases where it is very strong.

The relation theoretically derived, that link the power supplied and the wall shear stress is the well known expression:

$$E^2 = A + B\tau_w^n \qquad (1)$$

where A, B and n have to be determined from calibration.

The skin friction calibration has been carried out positioning each wire perpendicular to the channel flow and measuring the voltage E from a Dantec anemometer 55C System and the pressure drop along the channel to which is related the wall shear stress.

Typical skin friction calibration curves are shown in Fig.7 for two nominally identical probes, and in Tab.2 are reported typical values of the coefficients A, B and n.

From Fig.7 and Tab.2 it can be deduced that, also for this kind of probes, the curves are not identical due to the different interferences between the two wires and probably to the different positioning of the wires respect to their center cavities.

Probe	Wire	A	B	n
C	1	1.729	0.736	0.578
	2	1.563	0.877	0.552
E	1	1.761	0.550	0.548
	2	1.578	1.039	0.571

Table 2 - Hot-wire calibration coefficients.

For the directional response, two calibrations have been performed in terms of:

$$FT1 = \frac{(E_1 - E_{01}) - (E_2 - E_{02})}{(E_1 - E_{01}) + (E_2 - E_{02})}$$

and

$$FT2_1 = \frac{E_1 - E_{01}}{E_{max_1} - E_{01}}; \qquad FT2_2 = \frac{E_2 - E_{02}}{E_{max_2} - E_{02}}$$

where E_1 and E_2 are the voltages from the two wires, while E_{01} and E_{02} are the voltages corresponding to the no flow condition.

The functions $FT1$ and $FT2$ depend only on the angle δ between the wall shear stress and the axis of symmetry of the probe. These are shown in Fig.8, Fig.9 and Fig.10.

To proceed to the evaluation of modulus, direction and versus of the skin friction, once the voltages E_1 and E_2 are measured, is possible, using the function $FT1(\delta)$, to evaluate the direction δ, that is not a unique value. In fact the quasi sinusoidal behaviour of the $FT1(\delta)$ leads to more than one value of δ and the problem is insoluble.

The same problem seems there is also for the $F(\delta)$ function relative to the pressure block probes but, because of in that case there are three pressures, is possible by a simple comparison understanding in which sector to read the function.

In any case two of the four possible values are shifted just of 180° respect to the other, so the real unknowns are only two directions; further, comparing the two voltages, is also possible decide which of the two is the right direction. Remain without answer the versus, that could be determined from other guideline, for example following the evolution of the direction of wall shear stress starting from a point where sometime the direction is known (plane of symmetry of the flow field). Also a rough estimation of the direction is sufficient, in order to orient the probe axis in that direction (flow visualization). The first way has been followed by the authors to study a 3-D shear flow.

Once δ is known, $FT2(\delta)$ allows to calculate the voltages E_{max_1} and E_{max_2} that the two wires would have displayed if they had been placed perpendicular to the flow. The mean value is calculated from the two wall shear stress evaluated from the calibration curve corresponding to the two wires.

An analysis error of (1) leads to the following relation

$$\frac{d\tau}{\tau} = \frac{2}{n}\frac{E^2}{(E^2 - A)}\frac{dE}{E}$$

As it can be easily seen, in a non linearized system the error depends on the operating point on the calibration curve, and it increases remarkably at the lower range of the curve. The order of magnitude of the τ error is not less than 6% for a voltage error of 1%.

Analysing the calibration set of the two type of probes is deduced that even if different probes of the same type has similar behaviour, it is not possible to conclude that are universal calibration curves. This may be due to the fact that the more important the geometrical differences become, the greater is the geometric complexity: in fact the first and the main consequence of geometrical differences is the different interference. From this point of view is recommended to have great care in manufacturing probes of remarkable geometric complexity.

3. Application to a 3-D shear flow.

Inserting a circular cylinder between the channel walls has been generated a 3-D complex shear flow. The cylinder having a diameter of $88mm$ has been glued in a first step to the rotating disc, on which have been mounted four triangular pressure block probes, in four different circumferences and shifted 90° one respect to each other. By rotating the disc, that constituted part of the upper part channel wall, has been possible to perform detailed measurements of the wall shear stress on the channel wall around the cylinder.

In a second step, glueing the same cylinder to another disc instrumented with two hot-wire wall probes mounted in the same positions of two pressure block probes, the measurements have been performed. In Tab.3 are reported the probe positions and in Fig.11 the indication of the system disc-cylinder-probes with the angle convention in the measurement points. In particular θ is the angle between the channel axis and the wall shear stress.

	Probe	R[mm]	γ_{Probe}
Triangular Press. Probe	B	95	270°
	C	78	0°
	D	61	90°
	E	112	180°
Hot-wire Probe	C	78	0°
	E	112	180°

Table 3 - Probe positions.

The temperature influence was checked repeating calibration curves at different days and observing few percents of scatter under ambient temperature variations of ±2°, in any case skin friction calibration curves have been performed before and after the measurements.

The flow conditions have been fixed to have an upstream axis velocity of $11m/sec$, resulting in a channel and cylinder Reynolds number, respectively:

$$Re_{CH} = 29.000 \quad and \quad Re_C = 64.000$$

In Fig.12 and Fig.13 are displayed the comparisons of the evolution of the wall shear stress measured with the two kinds of probes, respectively for probe C and E, while in Fig.14 and Fig.15 is shown its direction evolution. In these diagrams γ is the angle to individualize the measurement point, shown in Fig.11.

At an higher velocity, $U_{axis} = 21m/sec$, measurements have been performed only with pressure block probes, because of the wall shear stress were outside their calibration curves; polar plot of the shear stress and oil flow visualization are shown in Figs. 16 and 17.

Finally evidence of flow unsteadyness is exhibited in Fig.18 for probe C and Fig.19 for probe E in terms of e_{RMS}. Further Fig.20 and Fig.21 shown the power spectrum density from probe E in two different angular positions $\gamma = 45°$ and $\gamma = 165°$ and $U_{axis} = 11m/sec$.

4. Comments

Starting from the results shown in Figs.12, 13, 14, 15, is evident that appear much more agreement between the direction of the wall shear stress, than the modulus. In particular, probe C (Fig.12) exhibits good agreement in a range of ±60° and then, even if the general behaviour is similar, there are some large differences. In fact the hot wire probe shows two maxima in each half part, the second one, at $\gamma = 140°$ or $\gamma = 220°$ and higher than the first, being in the rear part of the cylinder where strong vortical structures (horseshoe vortices) take place and, as a consequence, could induced high velocity gradient. This second peak of shear stress is not detected from the pressure probe, showing on the other hand the maximum higher of 10% compared with that of the hot-wire-probe.

These differences could be explained, thinking of the less global dimensions of the hot wire probe that means an higher spatial resolution and less flow disturbance, it acts as a quasi non intrusive sensor. On the contrary, the pressure probe can itself disturb the flow and further strong local pressure gradients, radial and tangential, can affect the pressure reading.

The good agreement in ±60° is also related to the absence of strong local pressure gradient.

The same situation is present in Fig.13 even if the data from the pressure probe in the half part $180° - 360°$ seems to be doubtful; good agreement is reached also in this case, from 0° up to 60°. Once again the hot wire probe reveals a second weaker peak of skin friction not shown from the pressure probe. To conclude, outside the range of $\gamma = \pm 60°$ the hot-wire measured wall shear stresses are more reliable, because of the non influence of the pressure gradient and because of the better sensitivity to capture every structure.

An overall picture of the vector shear stress for an higher velocity centerline, plotted in Fig.16, displays an accurate description of the wall flow field also very well confirmed from wall skin friction lines showed in the oil flow visualization, performed at the same Reynolds number. In fact some details of the typical horseshoe vortices, present around the cylinder, emerge from the measurements. The visualization, even if the Reynolds number is higher than that corresponding to Figs.12 and 13, shown vortical structure around the whole cylinder and in particular in its rear part. This could confirm the presence of the two peaks of wall shear stress present in Fig.12 and in Fig.13.

Same evidence of the unsteadyness in the flow field can be deduced from Figg.18 and 19. Very high fluctuations take place in the wake of the cylinder, where vorticity

is shedded and also wall interaction vortical structures are present; a peak of e_{RMS} is in fact present around $\gamma = 180°$.

The existence of the shedding phenomenon comes also from probe E; is clear the peak in the power spectrum density centered on 32 Hz that corresponds to a Strouhal number, based on the velocity centerline of $11m/sec$, equal to 0.25 higher than the Roshko *Strouhal – Reynolds number* results for 2-D cylinder in a free stream[16]. The present results shown that also in this case, with a very complex flow field around the cylinder, the basic shedding phenomenon is present and drive the unsteadyness effects. It means also that the Roshko's relation seems to be of a more general validity even for highly complex flows, as the present one, where the area ratio between cylinder and cross section is 0.314.

In this conditions, in fact, from the oil flow visualization seems that the two horseshoe vortical structures, one for each wall, are of the same order as the half height of the cylinder and could also interact between them, destroying the regular shedding, but in spite of this situation the phenomenon is still present.

This is a further confirmation that the alternate vortex street is a very stable condition and from many different kind of flows the situation collapses into the alternate wake.

This is not only true for unsteady flow, as in this case, but also in the steady case of yawed bodies[17], as observed many times. The reasons for this are not well understood up to now and require further investigations.

As it was expected the peak with his harmonic is much more intense in the wake (Fig.21) than in former part.

5. Conclusions.

Two different probes, triangular pressure block and hot-wire wall, have been calibrated in a channel. The first kind results to be really omnidirectional while an ambiguity arises from the second type, in knowing the versus of the wall shear stress. Neither for pressure probes nor for hot-wire probes seems that is extremely difficult to have a set of universal calibration curves in spite of great care has been observed in manufacturing the probes.

Measurements in a 3-D complex flow, generated in the same calibration channel, inserting a cylinder from wall to wall in the test section, have shown a good agreement between the results coming from the two type of probes, especilally for the direction; only in a restricted area ($\pm 65°$) of the former part the agreement is good also for the wall shear stress modulus; these are places where no strong pressure gradients are present.

More reliable are the measurements performed from the hot wire because of there isn't any effect of the pressure gradient.

The results shown also a better peculiarity of the hot-wire probe to put in evidence some characteristic structures, not revealed from the pressure probe, related to the higher resolution and to the less intrusivity.

Finally, good evidence of the unsteady effects is displayed from the hot-wire probe, showing that, even for this very complex flow, the shedding phenomenon is well established.

Acknowledgments

The authors are very grateful to Mr. A. Benedetto and Mr. R. Tassone for their technical assistance.

References

[1] *Skin friction drag reduction.* AGARD FDP/VKI Special Course, VKI Bruxelles, 2-6 March 1992.

[2] D.J.Peak, M.Tobak *Three-dimensional separation and reattachment.* AGARD Lecture Series, No.121, March 1982.

[3] V.C.Patel *Calibration of the Preston tube and limitations on its use in pressure gradient.* JFM, Vol.23, part.1, pp.185-208, 1965.

[4] K.G.Winter *An outline of the technique available for measurement of skin friction in turbulent boundary layer.* Prog. Aerospace Sci., Vol.18, pp1-57, 1977.

[5] H.Ludwieg *Ein Gerät zur Messung der Wandschubspannung turbulenter Reibungsschichten.* Ing-Arch. 17, pp.207-218, 1949.

[6] B.J.Bellhouse, D.L.Schultz *Determination of mean and dynamic skin friction, separation and transitional in low-speed flow with a thin-film heated element.* J.F.M., Vol.24, pp.379-400, 1966.

[7] H.U.Meier, H.P.Kreplin *Experimental investigation of the boundary layer transition and separation on a body of revolution.* Proc. of the 2th Symp. on Turbulent Shear Flows, London, 1979.

[8] M.J.Nituch, W.J.Rainbird *The use of geometrically similar obstacle blocks for the measurement of turbulent skin friction.* ARC 34423, 1973.

[9] P.Dexter *Evaluation of a skin friction vector measuring instrument for use in 3-D turbulent incompressible boundary layers.* Univ. of Southampton, Dept. of Astronautics and Aeron., Undergraduate Project, 1979.

[10] G.Iuso, M.Onorato *Skin friction measurements in 3-D boundary layers.* Int. Conf. on Experimental Fluid Mechanics, Chengdu, China, June 1991.

[11] G.Iuso, M.Onorato, P.G.Spazzini *Skin friction measurements in 3-D boundary layer.* 14th Int. Cong. on Instrumentation in Aerospace Simulation Facilities, Rockville-Maryland, USA, October 1991.

[12] S.DePonte, M.Parrini *A hot wire for detecting wall shear stress.* 14th Int. Cong. on Instrumentation in Aerospace Simulation Facilities, Rockville-Maryland, USA, October 1991.

[13] R.Houdeville, J.C.Juillen *Skin friction measurement with hot element.* VKI LS 05, 1989.

[14] G.Iuso, M.S.Oggiano, S.DePonte *3-D boundary layer measurements on an ellipsoid at angle of attack.* Int. Conf. on Fluid Mech., Beijing China, 1987.

[15] G.Iuso, M.Casella *Condotto fluidodinamico per la taratura di sonde di sforzo di attrito a parete.* Internal Report N.32, DIAS - Politecnico di Torino, 1990.

[16] A.Roshko *On the development of turbulent wakes from vortex streets.* NACA TN 2913, 1953.

[17] S.DePonte *Further studies on the asymmetrical flow past yawed cylinder.* ICAS 92, Beijing, September 1992

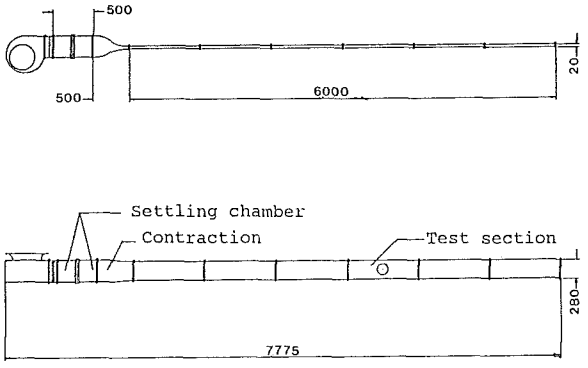

Fig.1 - Calibration channel. Dimensions in *mm*.

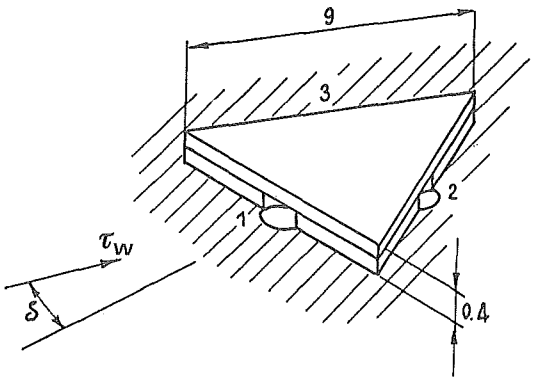

Fig.2 - Triangular block pressure probe for omnidirectional skin friction measurement. Dimensions in *mm*.

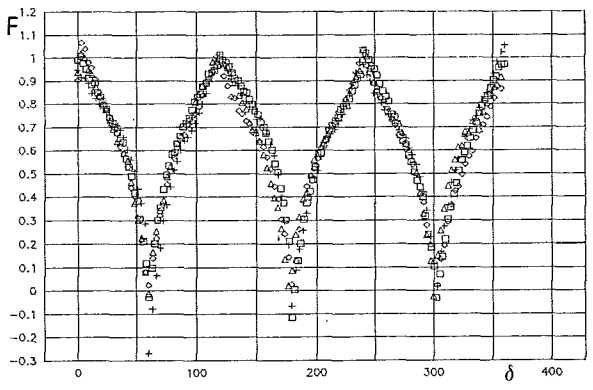

Fig.3 - $F(\delta)$ calibration function for triangular block pressure probe.

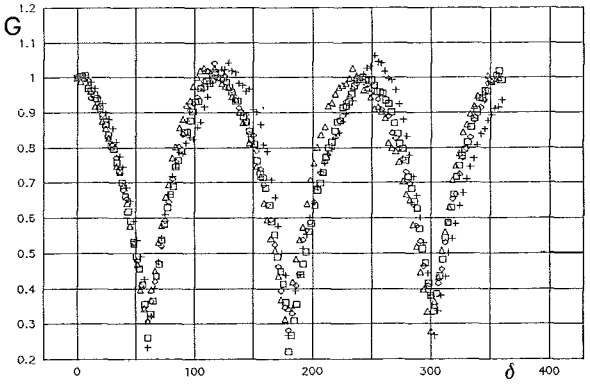

Fig.4 - $G(\delta)$ calibration function for triangular block pressure probe.

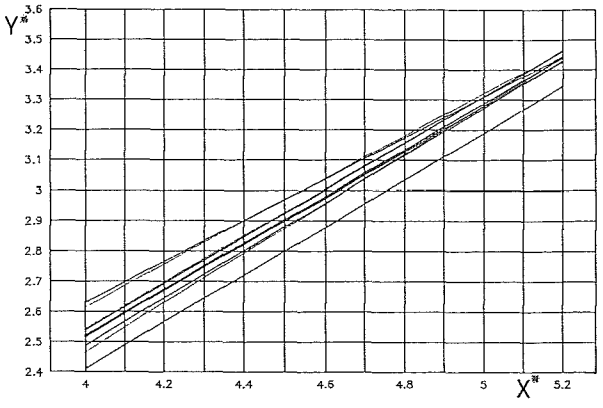

Fig.5 - $Y^* = Y^*(X^*)$ calibration function for triangular block pressure probe, for each probe side (1, 2, 3).

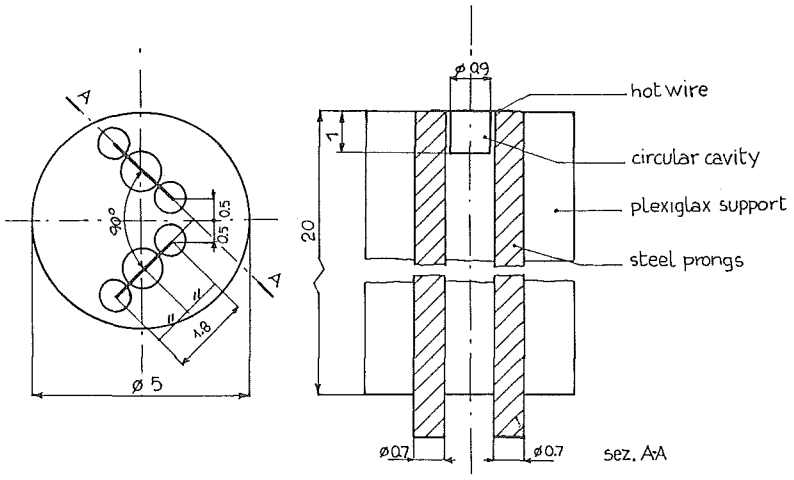

Fig.6 - Hot-wire wall probe. Dimension in *mm*.

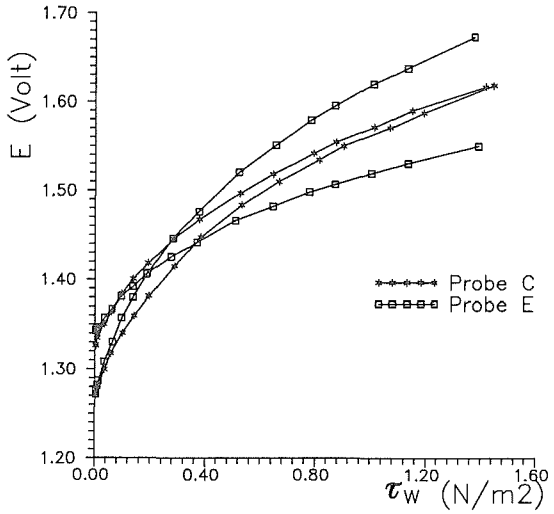

Fig.7 - Skin friction calibration curves.

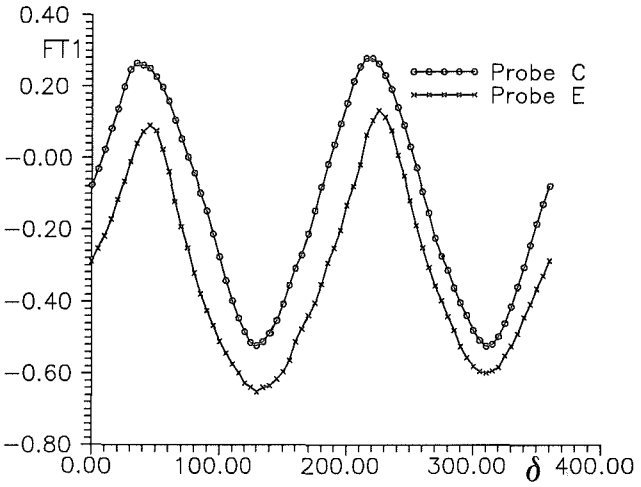

Fig.8 - $FT1(\delta)$ calibration function for hot wire wall probes.

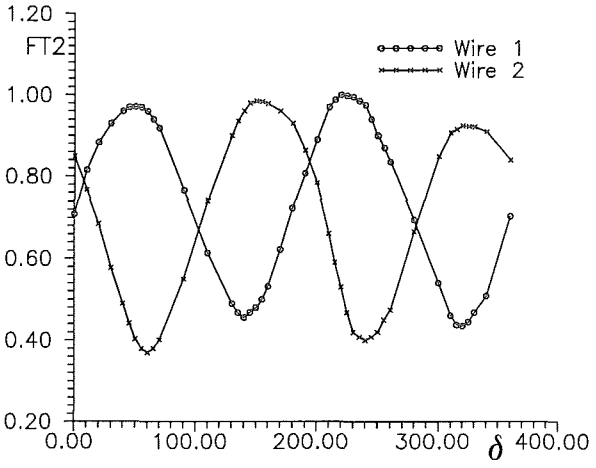

Fig.9 - $FT2(\delta)$ calibration function for hot wire wall probe E.

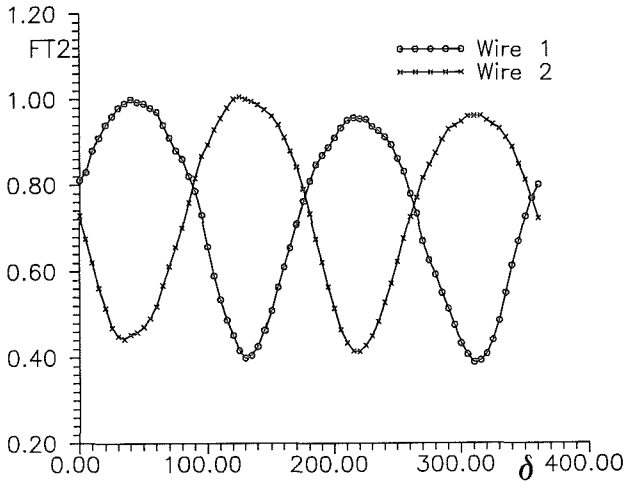

Fig.10 - $FT2(\delta)$ calibration function for hot wire wall probe C.

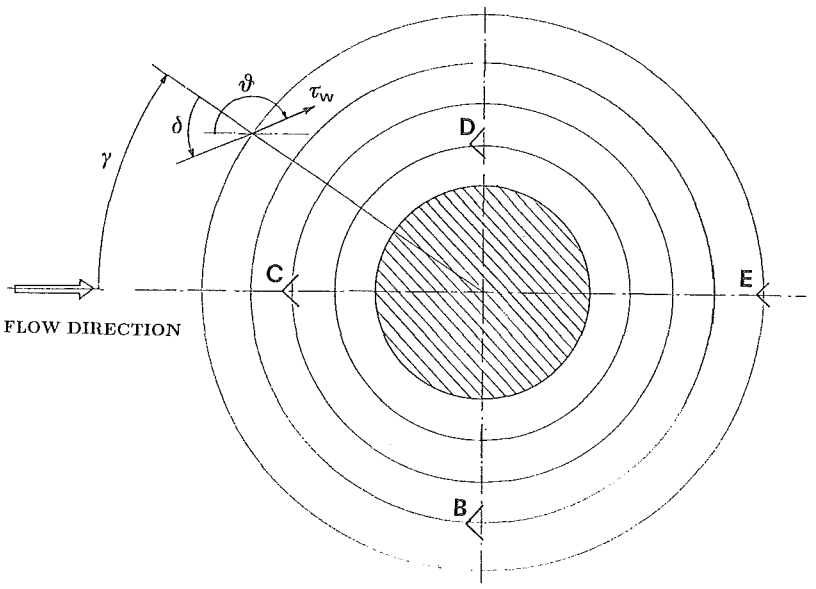

Fig.11 - Disc-cylinder-probes and angle's convention.

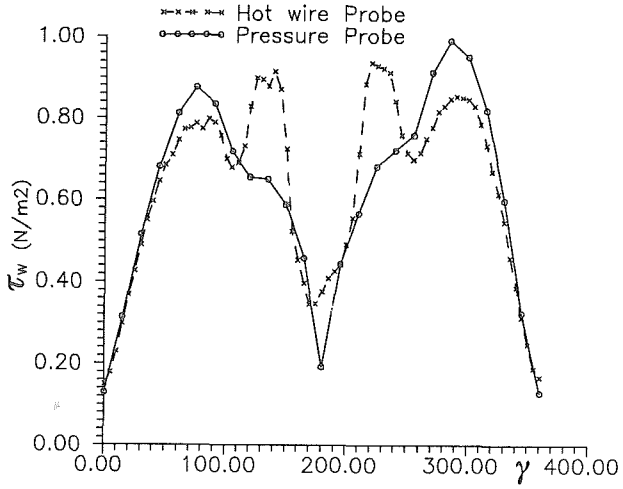

Fig.12 - Comparison of the evolution of the wall shear stress. Probe C.

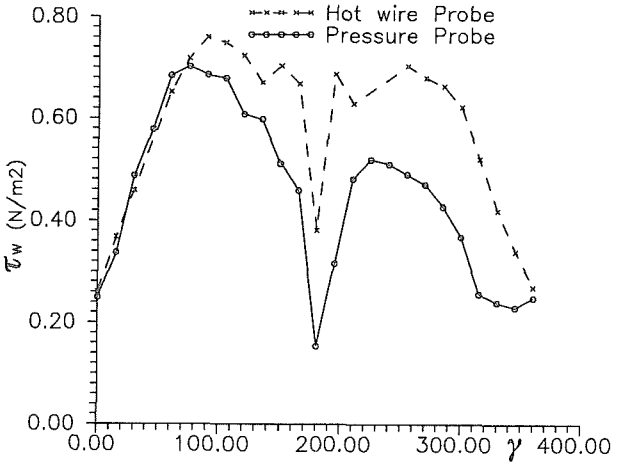

Fig.13 - Comparison of the evolution of the wall shear stress. Probe E.

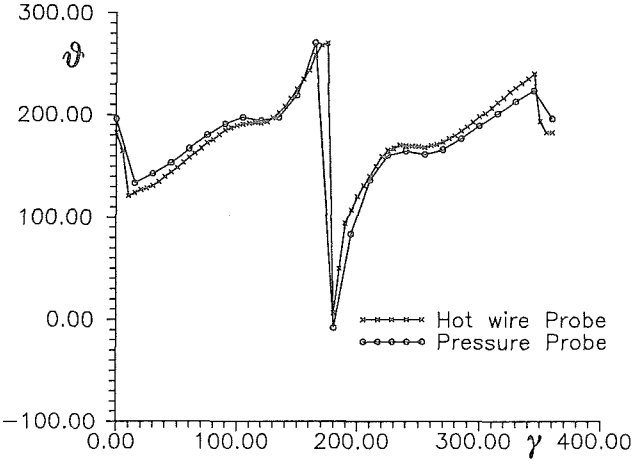

Fig.14 - Comparison of the direction evolution. Probe C.

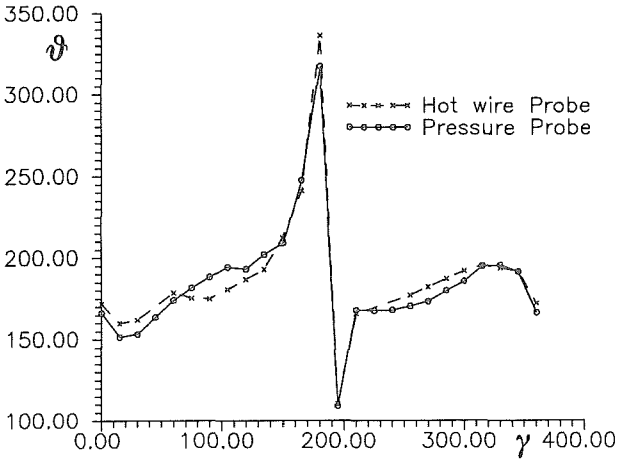

Fig.15 - Comparison of the direction evolution. Probe E.

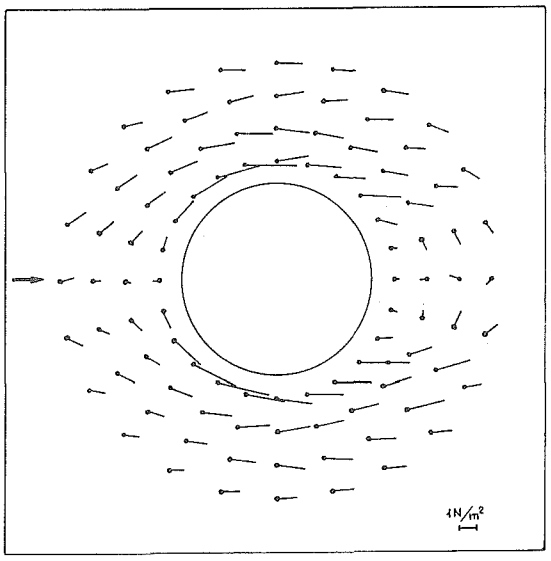

Fig.16 - Wall shear stress polar plot. Pressure block probes. $U_{axis} = 21m/sec.$

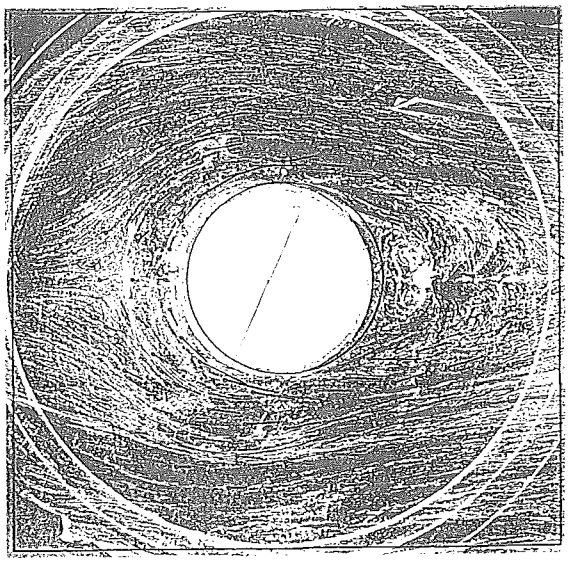

Fig.17 - Oil flow visualization referred to Fig.16.

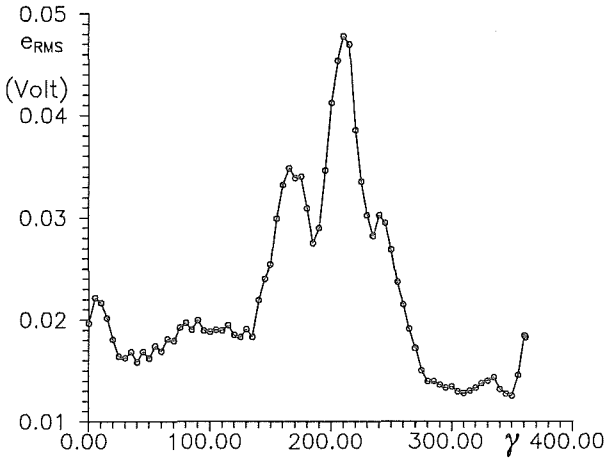

Fig.18 - Voltage fluctuations for probe C.

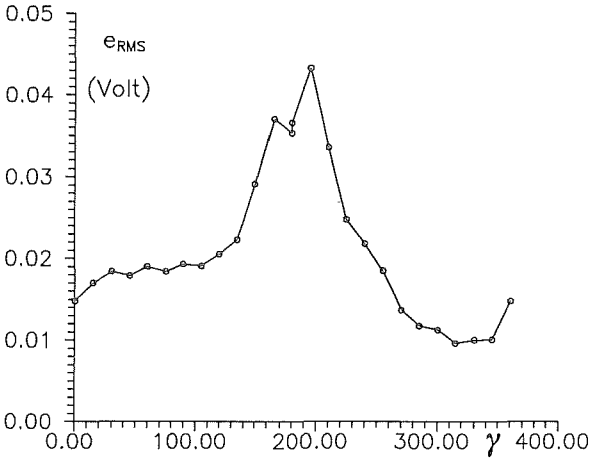

Fig.19 - Voltage fluctuations for probe E.

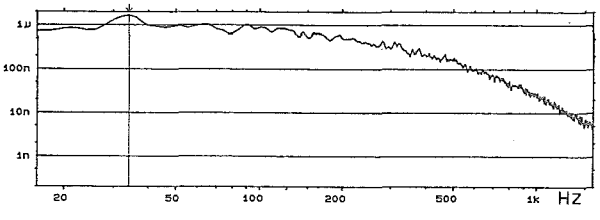

Fig.20 - Power spectrum density from probe E. $\gamma = 45^o$, $U_{axis} = 11m/sec.$

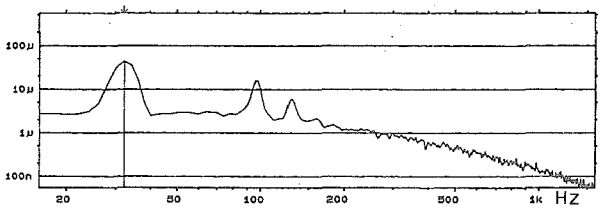

Fig.21 - Power spectrum density from probe E. $\gamma = 165^o$, $U_{axis} = 11m/sec.$